

ern Hemisphere. It is likely, however, that the aqueous-phase photoformation is also significant in the Southern Hemisphere.

The aqueous-phase photoformation of another oxidant, the hydroxyl radical ( $\cdot\text{OH}$ ), was also observed in authentic cloud and fog waters. The measured  $\cdot\text{OH}$  photoformation rates ranged from 0.44 to 5.3  $\mu\text{M hour}^{-1}$  in the four cloud and fog waters that were studied (7, 14). These rates are similar to the calculated fluxes of  $\cdot\text{OH}$  to atmospheric water drops from all other known sources (2, 3). Aqueous-phase photoformation of singlet molecular oxygen and unspiciated peroxy radicals have been reported previously (6), but the previous work did not demonstrate the formation of  $\text{H}_2\text{O}_2$  or any other peroxide.

In view of this additional source of  $\text{H}_2\text{O}_2$  and other oxidants to atmospheric water drops, tropospheric aqueous-phase oxidations must exert even more influence than has previously been recognized on the atmospheric chemical cycles of peroxides, ozone, sulfur, iron, and carbon. These oxidations will also influence the formation of  $\text{H}_2\text{SO}_4$ , which affects the magnitude of acid deposition and the postcloud aerosol characteristics and optical properties of the atmosphere. Photoreactions such as those reported here for clouds and fogs are also likely to be important sources of oxidants in other atmospheric hydrometeors, such as hydrated aerosols, rain, and dew, and also on wetted foliage.

## REFERENCES AND NOTES

1. J. Lelieveld and P. J. Crutzen, *Nature* **343**, 227 (1990).
2. T. E. Graedel, M. L. Mandich, C. J. Weschler, *J. Geophys. Res.* **91**, 5205 (1986).
3. W. L. Chameides, *ibid.* **89**, 4739 (1984).
4. D. W. Gunz and M. R. Hoffmann, *Atmos. Environ.* **A 24**, 1601 (1990).
5. G. L. Kok, K. Thompson, A. L. Lazrus, S. E. McLaren, *Anal. Chem.* **58**, 1192 (1986); C. N. Hewitt and G. L. Kok, *J. Atmos. Chem.* **12**, 181 (1991). Peroxides detected by the method of Hewitt and Kok include  $\text{HO}_2\text{H}$ ,  $\text{CH}_2(\text{OH})\text{OOH}$ ,  $\text{CH}(\text{O})\text{OOH}$ ,  $\text{HOCH}_2\text{OOCH}_2\text{OH}$ ,  $\text{CH}_3\text{OOH}$ ,  $\text{CH}_3\text{CH}(\text{OH})\text{OOH}$ ,  $\text{CH}_3\text{C}(\text{O})\text{OOH}$ ,  $\text{CH}_2(\text{OH})\text{CH}_2\text{OOH}$ ,  $\text{CH}_3\text{CH}_2\text{OOH}$ ,  $\text{CH}_3\text{CH}_2\text{CH}(\text{OH})\text{OOH}$ ,  $\text{CH}_3\text{CH}(\text{OH})\text{CH}_2\text{OOH}$ ,  $\text{CH}_2(\text{OH})\text{CH}_2\text{CH}_2\text{OOH}$ , and  $\text{CH}_3\text{C}(\text{O})\text{OO}(\text{O})\text{CCH}_3$ . The possible formation of other organic peroxides can not be precluded.
6. B. C. Faust and J. M. Allen, in *Effects of Solar Ultraviolet Radiation on Biogeochemical Dynamics in Aquatic Environments*, N. V. Blough and R. G. Zepp, Eds., WHOI-90-09 (Woods Hole Oceanographic Institution, Falmouth, MA, 1990), pp. 48-50; ———, *J. Geophys. Res.* **97**, 12913 (1992).
7. J. M. Allen, thesis, Duke University (1992).
8. Atmospheric waters and a chemical actinometer (2-nitrobenzaldehyde or valerophenone in distilled water) in Teflon- or glass-stoppered quartz containers were separately illuminated at 20°C with sunlight, simulated sunlight, or 313-nm light. The vast majority of these photolyses were carried out within 3 weeks of sample collection. Replicate photolysis studies showed that additional storage (in the dark at 2° to 10°C) of up to 2 weeks causes only small changes in peroxide photoformation

rates (−18 to +25%, mean = +0.8%). Controls indicate negligible peroxide formation in atmospheric waters kept in the dark and in illuminated rinse waters (a rinse water is distilled water that is sprayed onto the cloud or fog water collector and collected and handled identically to an actual sample). Filtration of the atmospheric waters (0.5- $\mu\text{m}$  Teflon) changed their photoformation rates by <15% relative to the same unfiltered samples. This suggests that particles >0.5  $\mu\text{m}$  were neither the dominant source nor the dominant sink of the photoformed peroxides. The initial peroxide formation rate was determined from the slope of a curve that was fit by least squares to a plot of peroxide concentration versus time. Quantum yields were calculated on the basis of the total absorbance of the atmospheric water at 313 nm. Wire mesh screens were used to adjust the irradiance of the simulated sunlight.

9. J. Kadlecik et al., *Winter Cloudwater Chemistry Studies Whiteface Mountain 1982-1984*, ASRC/SUNY Publication No. 1008 (Atmospheric Sciences Research Center, State University of New York, Albany, 1985); P. H. Daum et al., *J. Geophys. Res.* **92**, 8426 (1987).
10. K. J. Olszyna, J. F. Meagher, E. M. Bailey, *Atmos. Environ.* **22**, 1699 (1988); A. M. Macdonald et al., paper presented at the Seventh Joint Conference on Applications of Air Pollution Meteorology with Air and Waste Management Association, New Orleans, LA, 14 to 18 January 1991.
11. R. J. Charlson et al., *Science* **255**, 423 (1992); J. Lelieveld and J. Heintzenberg, *ibid.* **258**, 117 (1992); J. Langner, H. Rodhe, P. J. Crutzen, P. Zimmermann, *Nature* **359**, 712 (1992).
12. G. P. Ayers and T. V. Larson, *J. Atmos. Chem.* **11**, 143 (1990); X. Lin and W. L. Chameides, *ibid.* **13**, 109 (1991).
13. J. Langner and H. Rodhe, *ibid.*, p. 225.
14. We quantified the  $\cdot\text{OH}$  photoformation rate by monitoring the appearance of phenol from the  $\cdot\text{OH}$ -mediated oxidation of benzene, which was added

to the atmospheric water as a probe for  $\cdot\text{OH}$ .

15. For a given atmospheric water,

$$R_{\text{norm}} = \frac{\frac{d[\text{peroxide}]}{dt}}{\max \frac{d[\text{peroxide}]}{dt}}$$

where  $d[\text{peroxide}]/dt$  is the rate of peroxide photoformation for a series of experiments on one atmospheric water with different irradiances.

16. For the actinometer,  $j_{\text{norm}} = (j_A)/(\max j_A)$ , where  $j_A$  is the corresponding first-order rate constant for direct photolysis of the actinometer (2-nitrobenzaldehyde in distilled water) for the same series of experiments with the atmospheric water.
17. Measurements were normalized with a chemical actinometer to conditions of an isolated spherical water drop in a 100% clear sky at solar noon on 24 September 1990 in Durham, NC (solar zenith angle, 36°; elevation, 121 m).
18. We thank the following people for their assistance in this study: J. Kadlecik, J. Lu, R. MacDonald, V. Mohonen, B. Murphy, S. Roychowdhury, P. J. Spink, and S. Virgilio (Whiteface Mountain); C. Banic, G. A. Isaac, W. R. Leatch, and A. M. Macdonald (Ontario); A. Basabe, R. Cryer, and T. Larson (Washington); J. Galloway, B. M. McIntyre, J. Sigmon and P. Thompson (Shenandoah Park); V. Aneja and P. Blankinship (Mount Mitchell); C. Johnson and J. Seiber (California); G. E. Likens and K. C. Weathers (cloud water collector); G. Kok (speciation of peroxides); and C. J. Richardson (carbon analyzer). Supported by the National Science Foundation (Atmospheric Chemistry Program), the Andrew W. Mellon Foundation, the National Institutes of Health through the Duke Integrated Toxicology Program, and the Okinawa Prefectural Government Human Resources Development Foundation.

9 October 1992; accepted 4 January 1993

## Genetic Conversion of a Fungal Plant Pathogen to a Nonpathogenic, Endophytic Mutualist

Stanley Freeman and Rusty J. Rodriguez\*

The filamentous fungal ascomycete *Colletotrichum magna* causes anthracnose in cucurbit plants. Isolation of a nonpathogenic mutant of this species (path-1) resulted in maintained wild-type levels of in vitro sporulation, spore adhesion, appressorial formation, and infection. Path-1 grew throughout host tissues as an endophyte and retained the wild-type host range, which indicates that the genetics involved in pathogenicity and host specificity are distinct. Prior infection with path-1 protected plants from disease caused by *Colletotrichum* and *Fusarium*. Genetic analysis of a cross between path-1 and wild-type strains indicated mutation of a single locus.

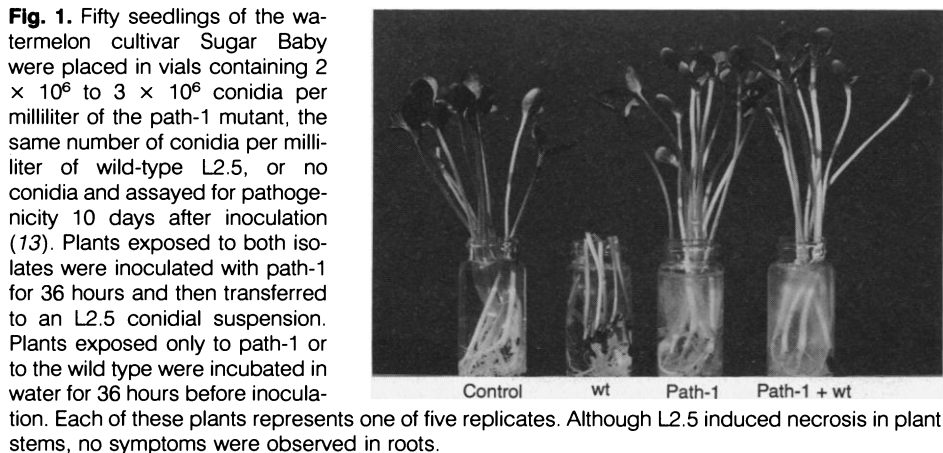
Filamentous fungal plant pathogens cause worldwide losses of billions of dollars and of millions of tons of agricultural produce annually (1). Use of chemical fungicides has led to the evolution of fungal resistance and to concern over the potential effects of these chemicals on other eukaryotes. Definition of the genetic and biochemical bases of fungal pathogenesis may lead to the

development of more effective, long-term, and ecologically safe fungal control strategies.

Fungal pathogenesis of host plants involves penetration of host tissue, host pathogen compatibility, dissemination through host tissue, induction of disease symptoms, and amplification of the pathogen by sporulation (2). The biochemical and genetic bases of host tissue penetration (3, 4), host compatibility (5, 6), and sporulation (7, 8) of fungal pathogens have been extensively studied. Here, we analyze a mutation in the process that allows pathogenic fungi to dis-

Department of Plant Pathology, University of California, Riverside, CA 92521.

\*Present address: National Fisheries Research Center, Building 204, Naval Station, Seattle, WA 98115.



seminate and cause disease in susceptible hosts.

Filamentous fungi from the genus *Colletotrichum* collectively infect the majority of agricultural crops grown worldwide (9). The species within this genus are hemibiotrophic pathogens (10) that begin the infection process when one of their spores adheres to host tissue and germinates to produce a germ tube. The germ tube differentiates to form an appressorium, which produces an infection peg that penetrates the first host cell. Host-pathogen compatibility is determined within the first infected plant cell. In a compatible interaction, the fungus grows through the first cell and mycelia disseminate through the host, leaving a path of necrotic tissue. In an incompatible interaction, the fungus ceases growth within the first cell and may elicit a hypersensitive response (11).

To analyze the genetics of host specific-

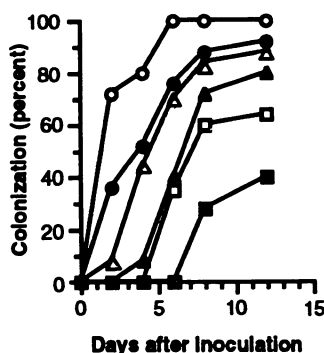


**Fig. 2.** Fifty seedlings of the watermelon cultivar Sugar Baby were inoculated with either path-1 or the wild-type L2.5 (Fig. 1). Every 2 days, five seedlings were surface sterilized with 1% NaOCl, sectioned into 3-cm pieces, plated on fungal growth medium (13), and assessed 3 days after plating. The open circles, triangles, and squares represent the growth of the wild type from the lower, middle, and upper sections, respectively. The closed circles, triangles, and squares represent the growth of path-1 from the lower, middle, and upper sections, respectively.

ity and fungal pathogenesis, we used a mutant of *C. magna* (12), path-1 (13), that was no longer capable of causing disease in cucurbit hosts. Watermelon seedlings were exposed to either the mutant path-1 or wild-type *C. magna* (Fig. 1). All of the plants exposed to wild-type *C. magna* expressed stem necrosis and died within 7 days after inoculation. However, no detrimental effects were observed in plants inoculated with path-1 that were monitored until flowering (~3 months).

To determine whether the mutation in path-1 had converted a compatible interaction to an incompatible one, a modification that would have likely involved host recognition of the pathogen (14), we monitored the extent of host colonization by path-1. Seedlings were surface-sterilized 14 days after inoculation, dissected into 3-cm sections, and plated on a fungal growth medium (13). Although the path-1 mutant was found throughout the entire seedling stem, a difference in the timing of colonization indicated that path-1 grew more slowly than wild type in host tissue (Fig. 2). In addition, path-1 was capable of growing past the cotyledon in the plant stem and was not isolated from leaf tissue (15).

Microscopic analysis confirmed that path-1 was able to infect the plants and

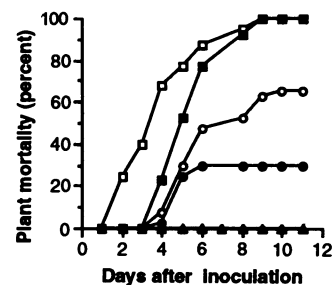


**Fig. 4.** Fifty seedlings of the watermelon cultivar Sugar Baby had their roots removed and were inoculated with either path-1 or the wild-type L2.5 (Fig. 1). At different times after inoculation with path-1, the cuttings were transferred to vials containing L2.5 conidia and assessed for mortality. The open and closed squares represent cuttings inoculated with L2.5 alone at time 0 or after 24 hours, respectively. The open and closed circles represent cuttings inoculated with path-1 for either 3 or 24 hours, respectively, followed by exposure to L2.5. The closed triangles represent plants inoculated only with path-1.

grow systemically within them, between the pith cavity and the outer cortex, in a way similar to the behavior of the wild-type strain. The wild-type and path-1 strains produced morphologically and functionally identical appressoria on the plant surface and within the plant tissue (Fig. 3), although appressoria have been thought to be involved only in penetration of the plant surface (16). We followed the systemic growth of both path-1 and wild type by monitoring the formation of appressoria inside the plants. Three days after infection, the number of appressoria and mycelia produced by path-1 was not significantly different from that produced by the wild type in the 2- to 4-cm zone above the inoculated roots. However, above 4 cm there was an inverse relationship between the number of appressoria and mycelia produced by path-1 and the distance from the roots, with fewer than ten appressoria observed in the 2-cm section above the cotyledon. The wild-type fungus produced the

**Fig. 3.** Seedlings of the watermelon cultivar Sugar Baby were exposed to either path-1 or the wild-type L2.5 (Fig. 1) for 4 days. Stem sections 3 cm above the inoculation point of each seedling were surface sterilized, longitudinally sectioned with a razor blade, and stained with cotton blue for light microscopic analysis. This section, which represents plant tissue between the central pith and the outer cortex, shows the formation of fungal appressoria (some are indicated by arrows) by path-1. Magnification bar, 20  $\mu$ m.

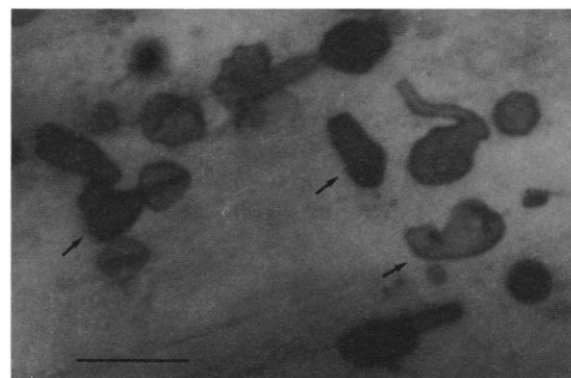


**Table 1.** Host range of the *C. magna* wild-type L2.5 and path-1. Plus signs indicate colonization; minus signs indicate no colonization. R, resistant reaction resulting in no mortality; S, susceptible reaction resulting in plant mortality; L, M, and U, lower, middle, and upper 3-cm sections of surface-sterilized seedlings.

Plant cultivar	Colonization						Disease reaction	
	L2.5			Path-1			L2.5	Path-1
	L	M	U	L	M	U		
<i>Dry beans</i>								
California dark red kidney	—	—	—	—	—	—	R	R
T39 (Black turtle soup)	—	—	—	—	—	—	R	R
<i>Cucurbits</i>								
Pumpkin (Jack-O-Lantern)	+	—	—	+	—	—	R	R
Squash (Burpee Golden Zucchini)	+	—	—	+	—	—	R	R
Cucumber (Burpee Pickler)	+	+	+	+	+	+	S	R
Cucumber (Poinsett 76)	+	—	—	+	—	—	R	R
Cantaloupe (Hale's Best Jumbo)	+	+	+	+	+	+	S	R
Watermelon (Charleston Grey)	+	+	+	+	+	+	S	R
Watermelon (Sugar Baby)	+	+	+	+	+	+	S	R
Watermelon (Crimson Sweet)	+	+	+	+	+	+	S	R
Watermelon (Jubilee)	+	—	—	+	—	—	R	R

same density of appressoria throughout the entire seedling before necrosis and death.

In all plants tested ( $n = 20$ ), path-1 was isolated from surface-sterilized tissue 6 to 10 cm above the inoculation zone 3 months after inoculation. However, unlike the wild-type fungus, path-1 did not sporulate in any of the plants. It has not yet been determined if path-1 can grow into fruit or if plant cultivars or species differ with regard to path-1 persistence. Nevertheless, because path-1 was not restricted to the first few cells of susceptible plants, it appears that the mutation did not simply convert a compatible interaction to an incompatible one. Thus a phytopathogenic fungus can be modified by mutation to grow as a nonpathogenic endophyte.

The wild-type fungus and path-1 were identical with regard to host specificity (Table 1). Both isolates were capable of systemic growth in all of the susceptible plants and incapable of colonizing resistant plants above the inoculation zone. However, the disease reaction remained distinct, with path-1 producing no visible effects on any plants. Thus, the loss of pathogenicity had no effect on host specificity.

The *C. magna* isolate DXDC that differed from path-1 in pathogenicity, mating type, pigmentation, and the presence of a resistance marker against chlorate was crossed with path-1 to determine the genetic complexity of the path-1 mutation (Table 2). The path-1 mutation segregated in a 1:1 ratio, which suggests that a single locus had been mutated. No linkage was observed between the path-1 mutation and either the resistance marker or pigmentation. It is therefore likely that the difference between path-1 and the wild type is the mutation of a gene or closely linked genes critical to the induction of disease after infection of the host.

Susceptible plants that were colonized with path-1 were protected from the virulent wt (Figs. 1 and 4). Protection was dependent on the extent of path-1 colonization before wild-type inoculation with exposures of 3, 24, and 36 hours to path-1 that resulted in 40, 70, and 100% reductions in mortality, respectively.

It is possible that protection of plants by path-1 resulted from the obstruction of the wild type from adhesion to specific infection sites. However, path-1 was also

**Table 3.** Protection of watermelon seedlings against *Fusarium oxysporum* f. sp. *niveum* (FON) by path-1.

Treatment*	Percent mortality†	
	Sugar Baby	Crimson Sweet
Water	0 c	0 c
Path-1	0 c	0 c
Water/FON	89 a	89 a
Path-1/FON	30 b	20 b
Path-1/FON‡	100 a	89 a

\*Nine seedlings were placed in vials containing  $2 \times 10^6$  to  $3 \times 10^6$  conidia per milliliter of path-1 for 7 days and then exposed to  $10^6$  conidia per milliliter of FON race 2 for 5 min before the seedlings were planted in vermiculite potting medium (22). Seedling mortality was assessed 21 days after inoculation, and treatments were performed in quadruplicate. †Values with a common letter were not significantly different ( $P = 0.05$ ). ‡Path-1 was killed by exposure to ultraviolet light.

able to protect the watermelon cultivars Crimson Sweet and Sugar Baby from disease caused by *Fusarium oxysporum* f. sp. *niveum*, which has a different mechanism of infection and dissemination than that of *Colletotrichum* (Table 3). In addition, both *Fusarium* and path-1 emerged from the inoculation zones of surface-sterilized plants that were protected against path-1, which indicates that both species infected. Therefore, it is more plausible that plant protection induced by path-1 involves the host defense systems. However, it seems unlikely that path-1 was continually stimulating host defenses because there was no evidence of necrosis or detrimental effects such as those that are seen when host defenses are fully activated (17, 18). It is possible that path-1 was "priming," or activating, only a portion of the host defenses, so that when the plants were exposed to the wild-type fungus there was no delay in the defense response.

A variety of problems associated with biological control strategies (19) may be avoided with the use of a biocontrol agent that can be maintained inside plant tissue. It may be possible to induce mutants similar to path-1 in various pathogenic fungi with either narrow or wide host ranges in order to infect and protect specific plant species from fungal disease.

Fungal life-styles can be either saprophytic, symbiotic, or a combination of the two (20). Although symbiotic associations can be either parasitic, mutualistic, or commensalistic, the genetic bases of these different life-styles remain enigmatic. The fact that a mutation at a single genetic locus can change the fundamental biological description of an isolate from a pathogen to a nonpathogenic endophytic mutualist warrants reassessment of certain hypotheses that concern fungal ecology and evolution. The use of such mutants as biocontrol agents to

**Table 2.** Segregation analysis of the path-1 mutation.

	Traits of parental isolates		Traits of progeny†		Segregation ratio of progeny
	DXDC*	Path-1			
Pathogenicity	+	—	84 +	74 —	1.15 +/-
Pigmentation	D	L	72 D	86 L	0.84 D/L
Chlorate	R	S	86 R	72 S	1.19 R/S
Mating type	A	B			

\*A chlorate-resistant mutant derived by spontaneous mutation of *C. magna* isolate DXD. Plus sign, pathogenic; minus sign, nonpathogenic; D, dark; L, light; R, resistant; S, sensitive. †Progeny were obtained from three perithecia derived from a cross of DXDC and path-1 established as described (21).

develop ecologically safe pest management strategies may have a considerable impact on future agricultural practices.

## REFERENCES AND NOTES

- G. N. Agrios, *Plant Pathology* (Academic Press, San Diego, ed. 3, 1988), pp. 3–39.
- R. N. Goodman, Z. Király, K. R. Wood, *The Biochemistry and Physiology of Plant Infectious Disease* (Univ. of Missouri Press, Columbia, 1986), pp. 29–38.
- R. C. Staples and V. Mako, *Exp. Mycol.* **4**, 2 (1980).
- A. A. Bell and M. H. Wheeler, *Annu. Rev. Phytopathol.* **24**, 411 (1986).
- S. Isaac, *Fungal-Plant Interactions* (Chapman & Hall, London, 1992), pp. 186–207.
- J. M. Daly, *Annu. Rev. Phytopathol.* **22**, 273 (1984).
- G. T. Cole, *Microbiol. Rev.* **50**, 95 (1986).
- K. R. Dahlberg and J. L. Van Etten, *Annu. Rev. Phytopathol.* **20**, 281 (1982).
- D. F. Farr, G. F. Bills, G. P. Chamuris, A. Y. Rossman, *Fungi on Plants and Plant Products in the United States* (American Phytopathological Society Press, St. Paul, MN, 1989).
- R. J. O'Connell and J. A. Bailey, in *Biology and Molecular Biology of Plant-Pathogen Interactions*, J. Bailey, Ed. (Springer-Verlag, Berlin, 1986), pp. 39–48.
- K. Erb, M. E. Gallegly, J. G. Leach, *Phytopathology* **63**, 1334 (1973).
- S. F. Jenkins, Jr., and N. N. Winstead, *ibid.* **54**, 452 (1964).
- S. Freeman and R. J. Rodriguez, *Plant Dis.* **76**, 901 (1992). Path-1 was originally designated HU25 and was derived from the wild-type isolate L2.5.
- A. J. Anderson, in *Physiology and Biochemistry of Plant-Microbe Interactions*, N. T. Keen, T. Kosuge, L. L. Walling, Eds. (American Society of Plant Physiologists, Rockville, MD, 1988), pp. 103–110.
- S. Freeman and R. J. Rodriguez, unpublished data.
- R. C. Staples and H. C. Hoch, *Exp. Mycol.* **11**, 163 (1987).
- M. R. Fernandez and M. C. Heath, *Can. J. Bot.* **64**, 648 (1985).
- E. W. B. Ward, in (10), pp. 107–131.
- J. W. Deacon, *Philos. Trans. R. Soc. London B* **318**, 249 (1988).
- H. J. Hudson, *Fungal Biology* (Arnold, London, 1986), p. 298.
- R. J. Rodriguez and J. L. Owen, *Exp. Mycol.* **16**, 291 (1992).
- S. Freeman and J. Katan, *Phytopathology* **78**, 1656 (1988).
- We thank N. Keen, R. Shaw, D. Ferrin, J. Menge, and G. Kurath for comments on the manuscript and R. D. Martyn for *Fusarium* isolates. Supported by grants from the United States-Israel Binational Agricultural Research and Development Fund (SI-0103-89) (S.F.), the University of California (UC) Regents, the UC, Riverside, Academic Senate, and the U.S. Department of Agriculture (9200655) (R.J.R.).

29 October 1992; accepted 12 January 1993

## Skn-1a and Skn-1i: Two Functionally Distinct Oct-2-Related Factors Expressed in Epidermis

Bogi Andersen, Marcus D. Schonemann, Sarah E. Flynn, Richard V. Pearse II, Harinder Singh, Michael G. Rosenfeld

Two forms of a member of the POU domain family of transcriptional regulators, highly related to Oct-2, are selectively expressed in terminally differentiating epidermis and hair follicles. One form, referred to as Skn-1i, contains an amino-terminal domain that inhibits DNA binding and can inhibit transactivation by Oct-1. A second form, Skn-1a, contains an alternative amino terminus and serves to activate cytokeratin 10 (K10) gene expression. The pattern of expression of the *Skn-1a/i* gene products and the effect of the alternative products on the expression of other genes suggest that these factors serve regulatory functions with respect to epidermal development.

Although skin is the largest organ in mature mammals, epidermal development begins only on embryonic days (e) 15 to 16 during rat development (1). Before this stage, the primordium of epidermis consists of a bilayer of cells, a superficial layer referred to as periderm that is later shed, and a basal layer (1, 2). On e16, the basal cells begin to proliferate, generating a stratified epithelium in which characteristic subsets of genes, such as keratins, are differentially regulated in each layer (1, 3). Most of

the suprabasal epidermal cells are postmitotic and eventually undergo programmed cell death, generating a superficial layer of dead cells (cornified epithelium) that appears on e18. This pattern of development, in which cells migrate to the surface during their differentiation only to undergo apoptosis, is continuously repeated in the adult, where the process is regulated by retinoic acid (4). Several transcription factors of wide distribution are expressed at high amounts in skin, including AP2, retinoic acid receptor  $\gamma$ , and retinoid X receptor  $\alpha$  (5). However, cell-specific transcription factors that may be involved in epidermal cell maturation remain unknown.

The cloning of *Pit-1*, *Oct-1*, *Oct-2*, and *unc-86* led to the discovery of a gene family characterized by a bipartite DNA binding

motif referred to as the POU domain (6–14). *Unc-86*, *Pit-1*, and *Oct-2* are believed to be important in the terminal differentiation of neuronal, pituitary, and B lymphocyte cell types, respectively (6, 7, 10, 11). *Oct-1* is a ubiquitous activator of gene programs required for cell proliferation (12) and may also play cell-specific roles (13). Subsequently, additional POU domain genes have been described in mammals, *Drosophila*, and *Caenorhabditis elegans*, most of which are transiently or selectively expressed in the developing nervous system (14).

Using screening by low stringency and polymerase chain reaction (PCR) of cDNAs from a number of tissues, we identified a cDNA clone distinct from known POU domain proteins (15). This cDNA clone contains a coding sequence predicting a 38-kD protein that is highly related to Oct-2 (Fig. 1). Whereas this protein differs from Oct-2 by only 15 amino acids over the POU-specific domain and the POU homeodomain, it is distinctly diverged from Oct-1 and Oct-2 in the linker region but contains regions of similarity outside the POU domain. To investigate the expression of this gene during development, we collected mouse embryos from blastocyst stage through e16.5, and PCR assays were performed by means of specific oligonucleotide primers (16) (Fig. 2A). This analysis revealed a biphasic pattern of expression: a signal was detected on e7.5, signal was low or undetectable between e9.5 and e12.5, and signal appeared again on e14.5. In addition, intense signal was observed in endometrium-placenta. In situ hybridization analyses with <sup>35</sup>S-labeled complementary RNA (cRNA) probe corresponding to the 3' untranslated region of the gene (17) revealed no hybridization in rat embryos corresponding to the early phase of expression. However, there was intense hybridization at e17 in epidermal structures throughout the embryo, with no specific detectable hybridization in any other region (Fig. 2B). Evaluation at higher resolution revealed a dense pattern of silver grains over the epidermis but not over the dermal structures, with the most intense hybridization consistently observed over the most superficial layer of the epidermis (Fig. 2C). In developing embryos, a single, superficial layer of cells, the periderm, revealed no hybridization, whereas the adjacent, underlying ectoderm revealed intense hybridization. A transcript of 2.3 kb was observed in RNA blots of skin from neonatal mice (18). Using the more sensitive ribonuclease protection assay, we confirmed expression in epidermis, but no signal was detected in RNAs from the following adult organs from mice and rats: skeletal muscle, tongue, esophagus, heart, thymus, spleen, liver,

B. Andersen, M. D. Schonemann, S. E. Flynn, R. V. Pearse II, M. G. Rosenfeld, Eukaryotic Regulatory Biology Program, Howard Hughes Medical Institute, University of California School of Medicine, San Diego, La Jolla, CA 92093.

H. Singh, Howard Hughes Medical Institute, University of Chicago, Chicago, IL 60637.